Effects of diffusion induced recrystallization on volume diffusion in the copper-nickel system

S.M. Schwarz *, B.W. Kempshall, L.A. Giannuzzi

Mechanical, Materials & Aerospace Engineering, University of Central Florida, Orlando, FL 32826, USA

Abstract

The effects of diffusion induced recrystallization (DIR) on volume diffusion in the Cu(Ni) system was investigated. Cu-Ni diffusion couples annealed at 500, 550, 600, and 650 °C for 120 and 200 h were used to calculate the volume diffusion for the Cu(Ni) binary system. Using characterization techniques such as focused ion beam (FIB) and transmission electron microscopy (TEM), observation of the interdiffusion zone revealed areas containing DIR and non-DIR. The volume diffusion of Ni into Cu across the non-DIR regions were calculated using the Boltzmann-Matano (B/M) method at 1 wt% Ni to be 8.05E-21, 9.88E-20, 4.53E-19, 2.67E-18 m²/s for 500, 550, 600, and 650 °C, respectively. Calculations of volume diffusion across the DIR zones were approximately three to four orders of magnitude higher than the volume diffusion based on the non-DIR information. Literature values for volume diffusion in the Cu(Ni) system are also higher than the non-DIR values by approximately one order of magnitude, implying that previous values may contain grain boundary contributions.
© 2003 Acta Materialia Inc. Published by Elsevier Science Ltd. All rights reserved.

Keywords: Volume diffusion; Diffusion of Ni into Cu; Diffusion induced recrystallization (DIR)

1. Introduction

Volume diffusion is one of many parameters used to determine mechanisms in solid state reactions such as creep, sintering, and phase transformations. Depending on the crystallographic structure, temperature, and other operating conditions, either volume or grain boundary diffusion may be the dominant mechanism for a particular solid state reaction. Thus, microstructure may play a significant role in diffusion processes.

Hart [1] first formulated a generalization of diffusion that included both volume and grain boundary diffusion contributions in polycrystalline material. Hassner [2] used Hart's formula to derive an effective diffusion coefficient as a function of volume and grain boundary diffusion coefficients as shown in Eq. (1).

$$D_{eff} = D_v + f D_b \qquad (1)$$

The variables D_{eff}, D_v, and D_b in Eq. (1) are defined as the effective, volume, and grain boundary diffusion coefficients, respectively; and f is a geo-

* Corresponding author. Tel.: +1-407-882-1500; fax: +1-407-2754-321.
E-mail address: smschwarz@yahoo.com (S.M. Schwarz).

metric constant. The coefficient f is further defined by the following equation.

$$f = k(\delta / l) \tag{2}$$

In Eq. (2), δ is the grain boundary width, l is the linear dimension of the grain, and k is $0.5 < k < 1.5$ depending on the geometry of the grain. Hence, the microstructure may play a significant role when calculating volume diffusion.

Volume diffusivities of Ni into Cu have been previously documented [3–7]. The techniques used to measure the concentration gradients from which volume diffusivities were determined included electron probe microanalyzer (EPMA), x-ray diffraction, and autoradiography. It is noted that these techniques may not provide microstructural information that may impact the calculation of volume diffusion.

According to Krishtal et al. [3] the effective diffusion, D_{eff}, which is dependent on both volume and grain boundary diffusion, as shown mathematically in Eq. (1), may identify how grain size affects the overall diffusion in polycrystalline materials. Krishtal et al. [3] have shown that from Cu-Ni diffusion couples annealed at 700 °C, volume diffusion is more predominant than grain boundary diffusion when the grain size is greater than 35 µm. Diffusion couples annealed at 800 °C showed volume diffusion is more predominant than grain boundary diffusion when the grain size is greater than 15 µm. They also showed that for 500 °C anneals, the effective diffusivity was dominated by grain boundary diffusion with a grain size as large as 80 µm. Krishtal et al. used a modified x-ray diffraction technique [8] to extract volume diffusion from the effective diffusivity of Ni into Cu. It should be noted that the microstructure of the Cu-Ni diffusion couples used in the experiments in references [3–7] were not characterized, and therefore, the type of interfacial microstructure cannot be confirmed.

Since the microstructure of the diffusion couples may play a crucial role in the determination of volume diffusion, the need to address the phenomenon of diffusion induced recrystallization (DIR) is of great importance. DIR has been well documented in the Cu-Ni binary system [9–12]. DIR is defined as the formation of new grains with different solute concentrations. The new grains are formed behind moving grain boundaries due to recrystallization as a result of the diffusion of solute atoms along the moving boundaries [9]. According to Liu et al. [12] the formation of DIR grains has been observed along a narrow region (the DIR zone) in the Ni substrate of a Cu-Ni diffusion couple at the original Cu-Ni interface. The diffusion couples used in the Liu et al. [12] experiments consisted of a polycrystalline Ni substrate electrodeposited on Cu and annealed at temperatures ranging from 550–900 °C. They report that three factors may be responsible for DIR: (1) the grain boundary Kirkendall effect, (2) the lattice Kirkendall effect, and (3) the coherency strain (the lattice mismatch) at the interface. In addition, Yamamoto and Kajihara [13] have recently proposed that an additional governing factor for DIR is the friction forces due to the solute drag effect of volume diffusion of solute into the untransformed matrix. Several sources have pointed out that new kinetic models describing the formation and growth of DIR is strongly influenced by the solute drag effect on grain boundary migration [9,13].

DIR has been observed as early as 1938 [14] and in many binary systems including Cu-Al [14], Cu-Ni [9–12], Cu-Si [14], and Cu-Zn [9,14–16]. From previous experiments performed in the Cu-Zn binary system [9,15,16], it was found that the magnitude and morphology of the DIR region was dependent on the surface finishing condition and the alloying concentration. In the Cu-Zn experiments, the copper single crystals were prepared by traditional mechanical polishing followed by a chemical polish. It was shown that DIR had a strong dependence on the amount of damage layer removed by the chemical polish. Thus, the propensity for DIR increased as the damage (i.e., coherency strain) increased. The experiments [16] also showed that the DIR region formed more extensively at higher annealing temperatures, longer annealing times, and higher Zn concentrations in the Cu-Zn alloy source.

DIR may enhance volume diffusion because the additional grain boundaries formed as a result of DIR will serve as faster diffusion paths than through the lattice. The importance of understanding the impact DIR may have on volume diffusion

is important when determining the mechanisms for solid state reactions. Thus, this paper reports on the influence of DIR on volume diffusion in the Cu-Ni system.

2. Experimental procedure

Cu crystals were first grown from 99.999% pure Cu using the vertical Bridgman technique [17]. A Buehler slow speed saw with a diamond wafer blade was used to section the crystals into specimens that were ~5 mm thick. The crystal samples were then mechanically ground using SiC papers of 400, 600, 800, and 1200 grit size, respectively. The crystals were then polished using 5, 1, and 0.3 µm alumina on a low-nap polishing pad. The samples were then electropolished in an attempt to remove any surface impurities or damage from the previous grinding and polishing steps. The electropolish was carried out at a potential of ~3 volts and a current of ~500 mA for ~60 s in an electrolytic solution of a 1:1 by volume mixture of phosphoric acid and de-ionized water. The single crystal Cu samples were then electroplated with approximately 75–125 µm of Ni to provide for an infinite or constant source during the subsequent diffusion anneals. Each sample was encapsulated in a Pyrex tube under an Ar atmosphere of ~350 mm Hg, placed in a furnace, and diffusion annealed at 500, 550, 600, and 650 °C for 120 or 200 h.

The Boltzmann-Matano (B/M) method was used to quantify the volume diffusion of Ni into Cu. The B/M method is a graphical means of interpreting volume diffusion from a concentration versus depth profile [18,19]. A plot of concentration versus depth is then constructed from which the volume diffusion is extracted. Hence, the information of interest is the concentration gradient of Ni in the region across the Cu-Ni interface.

Various techniques have been used to collect concentration data in diffusion couples. Since the diffusion lengths were deemed to be too small for bulk sample analysis, the concentration gradient of Ni across the interdiffusion zone was determined using (scanning) transmission electron microscopy ((S)TEM). When coupled with an X-ray energy

dispersive spectrometer (XEDS), the (S)TEM can perform semi-quantitative x-ray microanalysis. The determination of Ni across the Cu-Ni interdiffusion zone was performed using an FEI/Philips Tecnai F30 (S)TEM operating at 300 keV. Hence, electron transparent specimens were prepared for STEM/XEDS analysis.

A Focused Ion Beam (FIB) workstation was used to prepare site-specific TEM specimens across the Cu-Ni interdiffusion zone. First, the samples were mechanically ground and polished as outlined earlier. The in-situ FIB lift-out (LO) technique was used to obtain site-specific TEM specimens. An FEI 200TEM FIB workstation equipped with an Omniprobe in-situ tungsten (W) lift-out probe was used. The in-situ LO (INLO) FIB technique is adapted from both the traditional FIB method and the ex-situ LO method [20,21]. Using the INLO FIB technique, a bulk TEM sample is first milled in a wedge shape approximately 150 µm long by 5 µm wide by 5 µm deep. Note that the dimensions of these specimens are ~10 times longer than the conventional FIB/TEM specimens. Thus, each specimen took approximately four hours of FIB time to prepare it to electron transparency. The W LO probe is then attached to the specimen by ion beam assisted Pt chemical vapor deposition (CVD). The TEM specimen is then lifted from the bulk using the W probe as shown in a. Before the specimen can be adhered to the TEM grid, a 2 × 1 mm slotted Mo TEM grid is cut in half and positioned on the sample stud. A Mo grid was used to avoid x-ray energy overlaps with Cu and Ni.

After the sample is lifted-out, the grid is moved into the field of view. The probe is lowered to the TEM grid and the sample is fastened to the grid using the ion beam Pt CVD. Once the specimen has been attached to the TEM grid, the in-situ W probe is FIB milled free. The FIB is then used to thin the specimen to electron transparency (100–300 nm) as shown in Fig. 1(b).

The STEM was operated at 300 keV with a beam diameter of 4 nm FWHM. The STEM images were acquired using a Fischione high angle annular dark field (HAADF) detector located in the 35 mm port of the TEM. In some cases, the HAADF was operated in bright field mode in order
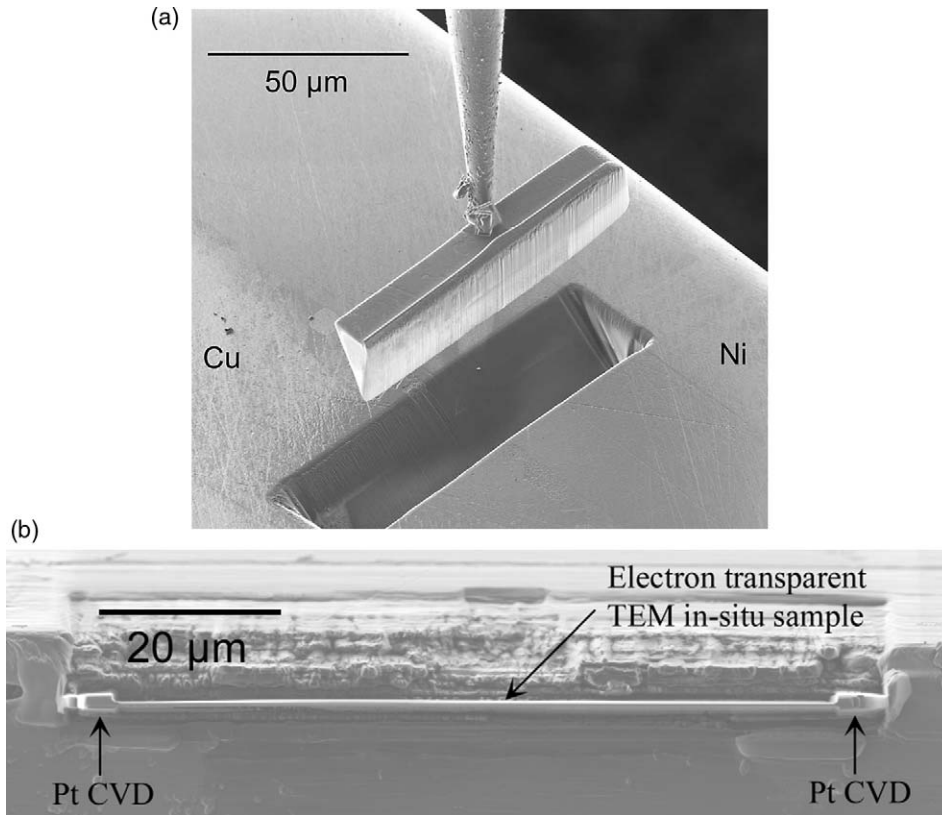
Fig. 1. The in-situ FIB lift-out technique from a Cu-Ni diffusion couple showing (a) the removal of the sample from the bulk material and (b) the specimen thinned to electron transparency using the FIB. Note the large dimension of this lift-out specimen (>80 μm) compared to conventional lift-out dimensions (~10–30 μm).

to obtain an image of the entire field of view of the large specimen. An EDAX detector with an energy resolution of 140 eV and a take off angle of 18° was used for the XEDS analysis. Each specimen was titled 0° toward the detector during analysis. Spectra were collected at 1 μm intervals with a dwell time of 5 s per point over a 100 μm length. The characteristic x-rays of $Cu_{K\alpha}$ at 8.047 keV and $Ni_{K\alpha}$ at 7.472 keV were used for quantification. Since the energy resolution of the XEDS detector is about 140 eV, there was no peak overlap between the $Cu_{K\alpha}$ and the $Ni_{K\alpha}$ x-rays. The quantification of the Ni in the Cu was performed from the standard Cliff-Lorimer equation [22] in Eq. (3).

$$\frac{C_A}{C_B} = k_{AB}\frac{I_A}{I_B} \tag{3}$$

In Eq. (3), C_A and C_B are the relative elemental concentrations within the interdiffusion zone of the diffusant and matrix respectively. I_A and I_B are the respective integrated x-ray intensities above the background, and k_{AB} is the sensitivity or k-factor for the two elemental species. The k-factor is instrument specific and it is therefore necessary to determine the k-factor specifically for the TEM and conditions used in this research. Thus, three Cu-Ni standards of varying concentrations (Cu 29.3 wt% Ni, Cu 50.4 wt% Ni, and Cu 67.6 wt% Ni as determined by inductively coupled plasma spectrometer) were manufactured and used to determine the k-factor between the $Cu_{K\alpha}$ and the $Ni_{K\alpha}$ radiation. Using INLO FIB specimens from the three Cu-Ni standard alloys, the k-factor at zero thickness, k^0_{NiCu}, was determined from the average of the three alloys to be 0.847 ± 0.198. For the analysis of the Ni diffusion in the bicrystals, the

thickness of the LO specimens was determined using the CBED method [23] and the corresponding ZAF correction factor (atomic number effect, x-ray absorption effect, and x-ray fluorescence) was calculated but found to be negligible (<1%) for the Ni concentration calculations. Thus, the zero thickness k-factor, k^0_{NiCu}, was used in quantifying the Ni concentration gradients across the interdiffusion zone.

Once the Ni concentration gradients were determined and plotted, a trendline was fitted to the concentration versus depth data and a B/M plot was constructed. The Matano interface was located and the volume diffusion (i.e., chemical diffusivity) was calculated as a function of concentration. The values chosen to represent the intrinsic diffusion, D, for each diffusion annealing temperature (500, 550, 600, and 650 °C) were taken at a Ni concentration of 1 wt%. Finally, the activation energies and the diffusion coefficients were calculated from the Arrhenius relation of log D versus $1/T$, where the slope of the line gives the activation energy and the diffusion coefficient is given by the intercept as $1/T \rightarrow 0$.

3. Results

Examination before diffusion annealing revealed that the Ni plated epitaxially onto the Cu single crystal substrate. Fig. 2(a) and (b) are FIB images of the cross-section of the pre-annealed sample showing the epitaxial deposition of the plated Ni onto the Cu crystal. The epitaxial nature of the Ni on the Cu is confirmed using two different tilt conditions in the FIB as shown in Fig. 2(a) and (b). The Ni and the Cu show the same relative contrast in both images indicating that their orientation is similar. In addition, no polycrystalline grain contrast is observed in either the Cu or Ni further indicating the single crystal nature of each phase. This is important when compared to the FIB images of an annealed sample where DIR is observed to occur at the Cu-Ni interface as shown in Fig. 3(a) and (b). Fig. 3(a) was obtained at a stage tilt of 0° and Fig. 3(b) was obtained at a stage tilt of 10°. Note the polycrystalline channeling contrast that is evident at the Cu-Ni interface. This sample was
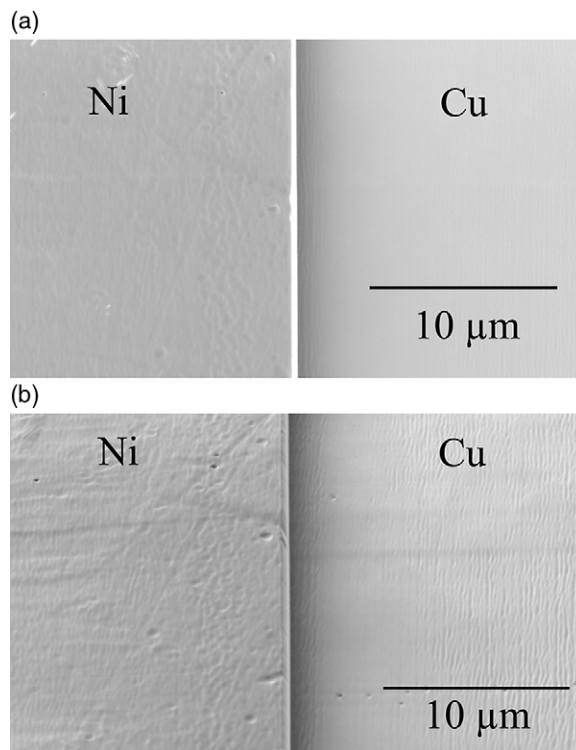

Fig. 2. FIB images of the Ni plated Cu samples at (a) 0° and (b) 50° stage tilts. The consistent change in contrast between images indicate that both the Cu and Ni are single crystal regions in this field of view.

briefly electropolished prior to FIB observation and thus the Cu side of the couple was observed to be preferentially removed.

The five diffusion couples, one annealed at 600 °C for 120 h and four annealed for 200 h at 500, 550, 600, and 650 °C, were further analyzed for DIR. The sample that was diffusion annealed for 120 h at 600 °C showed regions of DIR and regions devoid of DIR along the interdiffusion zone, as shown in Fig. 4. The sample shown in Fig. 4 was mechanically ground and polished, but not electropolished, as outlined earlier to prepare a relatively flat surface for INLO TEM specimens across the interdiffusion zone. The other four samples also showed similar results with most of the interdiffusion zone experiencing DIR and smaller portions of the interdiffusion zone devoid of DIR.

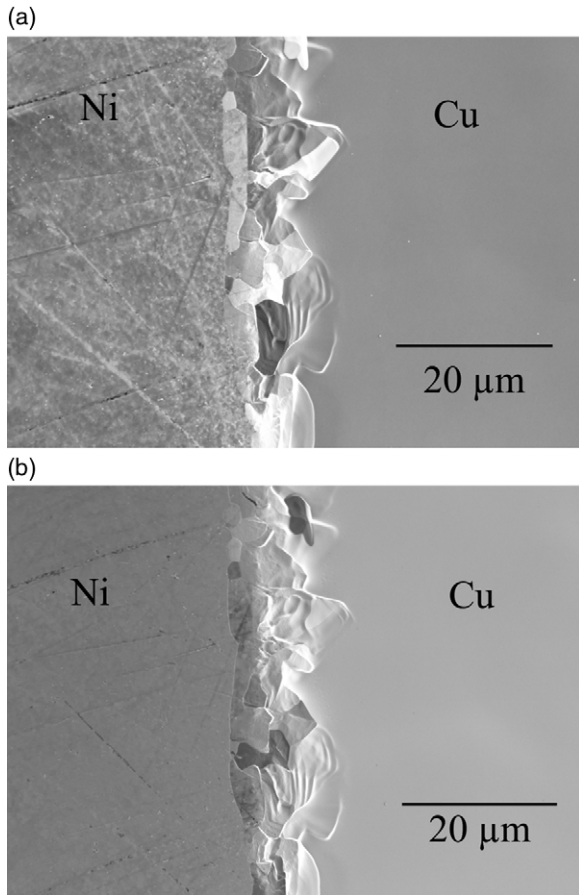From the STEM XEDS analysis, the concen-

(a)

(b)

Fig. 3.   FIB images indicating DIR at the Cu-Ni interface after annealing for 120 h at 600 °C obtained at a stage tilt of (a) 0° and (b) 14°. Note the presence of polycrystalline grains at the Cu-Ni interfacial region.
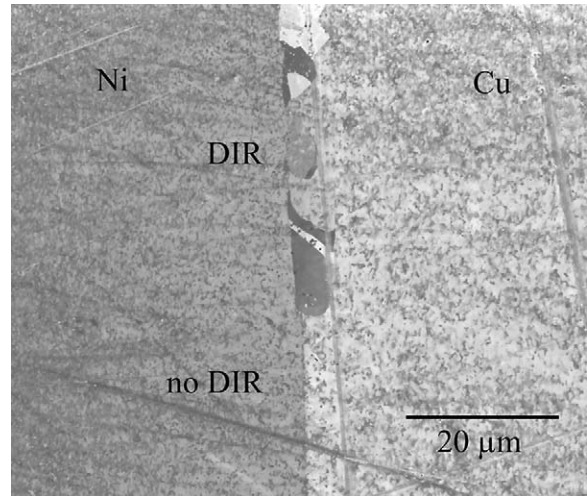

Fig. 4.   FIB image of Cu-Ni diffusion couple annealed at 600 °C for 120 h showing areas of DIR and areas devoid of DIR.
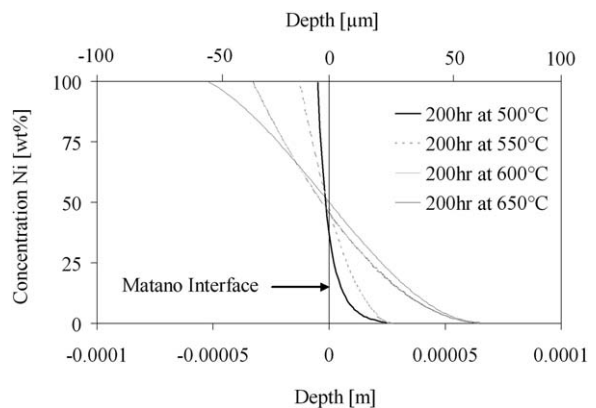

Fig. 5.   Comparison of B/M plots from Cu-Ni diffusion couples that experienced DIR annealed at 200 h for various temperatures. The Matano interface is also shown.

tration of Ni was plotted as a function of penetration depth. Then the B/M interface [18,19] was located and the chemical diffusivity, $\tilde{D}(c)$, was calculated using Eq. (4) [18,19].

$$\tilde{D}(c) = \left(-\frac{1}{2t}\frac{dx}{dc} \right)_c \int_{c_r}^{c} (x - X_M)\, dc \qquad (4)$$

A comparison of the B/M plots from the DIR samples is shown in Fig. 5. As expected, the B/M plots elongate with an increase in diffusion anneal temperature. Note that in all cases, the diffusion of Ni on the Cu rich portion of the interface occurs more gradually, while the diffusion of Cu into the Ni rich portion of the interface is more abrupt.

Fig. 6 is a plot of the chemical effective diffusivity of Ni into Cu as a function of Ni concentration for the Cu-Ni couples annealed from 500–650 °C. In Fig. 6, the chemical diffusivity is denoted as $\tilde{D}_{eff}$ since grain boundary effects due to DIR are known to be present. Note that the change of $\tilde{D}_{eff}$ with [Ni] shows an anomalous slope for the case where $T = 500$ °C, and to a lesser extent, $T = 550$ and 600 °C. This is due to the large errors that are inherent in calculating the B/M values at low concentration values. From Darken's equation,
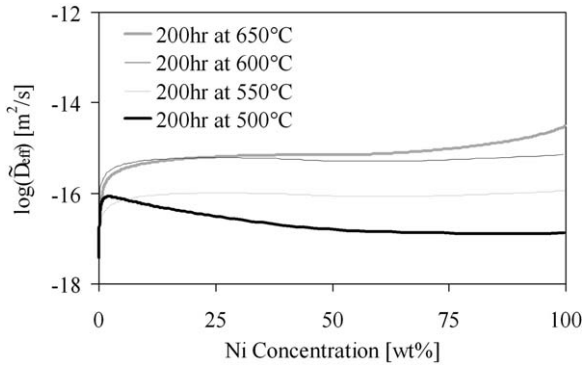
Fig. 6.   The effective diffusivity of Ni plotted as a function of concentration in the Cu-Ni system where DIR was observed.

shown below as Eq. (5), the intrinsic diffusivity is found at the limit when $N_{Ni} \approx 0$, and thus, $\tilde{D} \approx D_{Ni}$. It is understood that the B/M analysis may be associated with large errors at concentration levels at the extremes (very low [Ni] or very high [Ni])[14,24]. Since little confidence can be placed in the accuracy of the computed diffusivities at the extremes (i.e., $N_{Ni} \approx 0$) we have chosen a value of 1 wt% Ni to calculate the intrinsic diffusivity for the purpose of comparison to previous reports. Thus, the intrinsic volume diffusion of Ni into Cu was determined using Darken's equation at a concentration of 1 wt% Ni and the results are shown as an Arrhenius plot in Fig. 7. Note the poor fit to the data points which may be attributed to variation
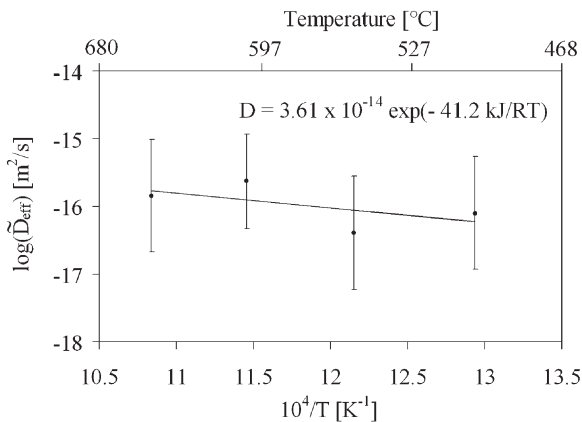

Fig. 7.   An Arrhenius plot of volume diffusion determined from the B/M method calculated at D_{eff} = 1 wt% Ni obtained where DIR was observed to occur.

in grain structure as a result of DIR within each sample [25].

$$\tilde{D} = N_{Cu}D_{Ni} + N_{Ni}D_{Cu} \tag{5}$$

Further investigation was performed on the Cu-Ni diffusion couple annealed at 600 °C for 120 h to show the influence DIR may have on bulk diffusion. TEM specimens were prepared from both the DIR and non-DIR regions using the INLO procedure as outlined earlier. The TEM images of the DIR and non-DIR regions and concentration plots obtained from STEM/XEDS scans are shown in Fig. 8(a)–(c), respectively.

XEDS was performed using the STEM on the two specimens shown in Fig. 8(a) and (b). The presence of grains between the Cu and Ni regions is evident in Fig. 8(a). A distinct interfacial region is evident in the region without DIR as shown in Fig. 8(b). Plots were constructed from the XEDS profiles and a comparison of the concentration/depth profiles from the DIR and non-DIR regions is shown in Fig. 8(c). The difference in the B/M plots clearly shows an increase in diffusion through the bulk in the DIR case as a result of the newly formed grain boundaries. The difference in diffusion lengths between the DIR and non-DIR regions is approximately one order of magnitude. Clearly, DIR is a major factor that influences diffusion through the bulk and may produce volume diffusion results that are overestimates of the ideal volume diffusion values.

It was noted that the concentration profile associated with the DIR region shown in Fig. 8(c) revealed areas of discontinuities that coincide with grain boundary positions in the corresponding TEM image. The initial drop-off in the DIR concentration profiles is due to volume considerations (as per the non-DIR example shown in Fig. 8(c)). All other discontinuities and deviations in the profiles may be attributed to the location of grain boundaries and/or other crystalline defects. This may be shown schematically in Fig. 9 where the relative sizes of the arrows denote relative amounts of material transfer. A grain boundary will act as a sink for all atoms approaching it. More atoms will diffuse along the boundary than across the boundary. This has a net effect of elongating the concentration profile in the B/M type of curve.
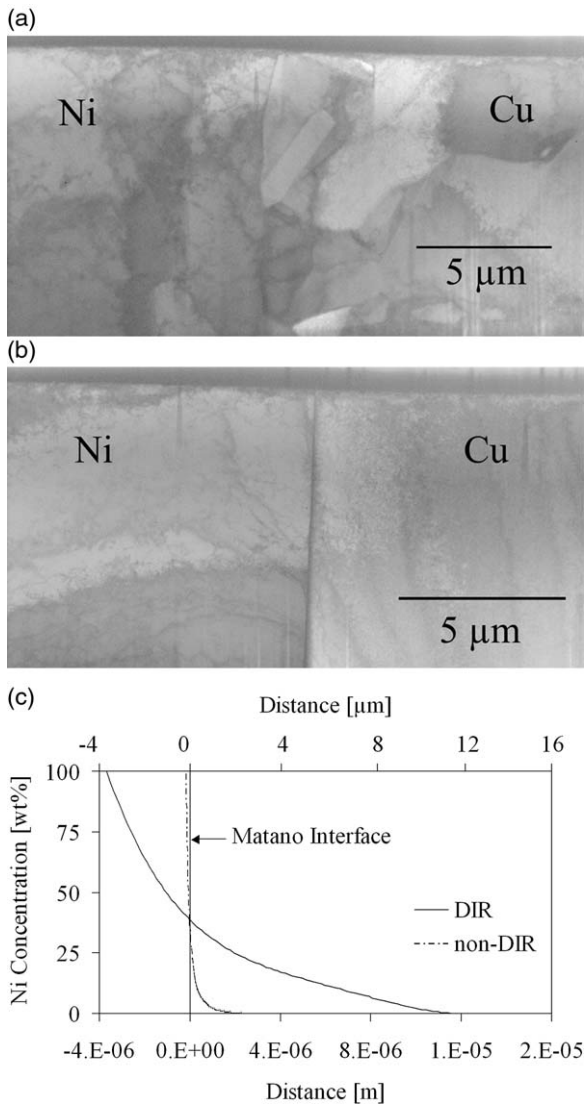
(a)

(b)

(c)

Fig. 8. BF TEM images from (a) DIR and (b) non-DIR regions of Cu-Ni diffusion couple annealed at 600 °C for 120 h used to construct and compare (c) B/M plots obtained from STEM/XEDS scan. Note the large differences in diffusion lengths observed between the DIR and non-DIR regions due to grain boundary contributions.

Note that the size of a discontinuity may be consistent with grain boundary structure (or other crystallographic defect). For example, the concentration profile across a coherent twin boundary does not vary significantly. This is expected, since minimal diffusion is expected along a coherent twin boundary. Thus, local fluctuations of concentration are observed (as evident by Fig. 8(c)) depending on the specific defect contributions.

Since the DIR and non-DIR results previously presented showed large variations, an effort was made to locate regions along the diffusion couples annealed at additional temperatures where no DIR took place. Non-DIR regions were found in samples annealed at 500, 550, and 650 °C for 200 h each. These regions were prepared using the FIB INLO technique as described before. In each of the profiles little or no detectable Cu was observed to diffuse into the Ni side of the couple, an example of this is shown in Fig. 10. Using the conditions and techniques in this study, the volume diffusion results indicate that the chemical D for Cu into Ni, $\tilde{D}_{Ni(Cu)}$, is less than $\tilde{D}_{Cu(Ni)}$ which agrees with previously reported work [26–33].

The B/M method was used to determine the intrinsic diffusion of Ni into Cu for each non-DIR sample at a Ni concentration of 1 wt%. The results are shown in the Arrhenius plot in Fig. 11. From the Arrhenius plot in Fig. 11, $D_o = 1.52 \pm 0.17$ E-5 m^2/s, and $Q = 225 \pm 25$ kJ. Note also the remarkable correlation that exists between the data, compared to the large deviation in effective diffusivity data previously shown in Fig. 7 due to grain boundary effects. Thus, the non-DIR data provides an apparent "true" value for the volume diffusion of Ni into Cu. The non-DIR data is compared to all known previous data as shown in Fig. 12. As evident by Fig. 12, the values for the "intrinsic" (or effective) diffusion of Ni into Cu obtained for the samples which did not exhibit DIR show the lowest values, indicating the possibility that grain boundary effects have contributed to previous diffusivity values.

4. Discussion

The importance of understanding the DIR phenomenon and how it may influence volume diffusion calculations is evident in terms of the fundamentals of grain boundary diffusion. The transport of material is faster down grain boundaries than through the crystal or bulk [34]. If DIR is the manifestation of grain boundary diffusion, then calculat-
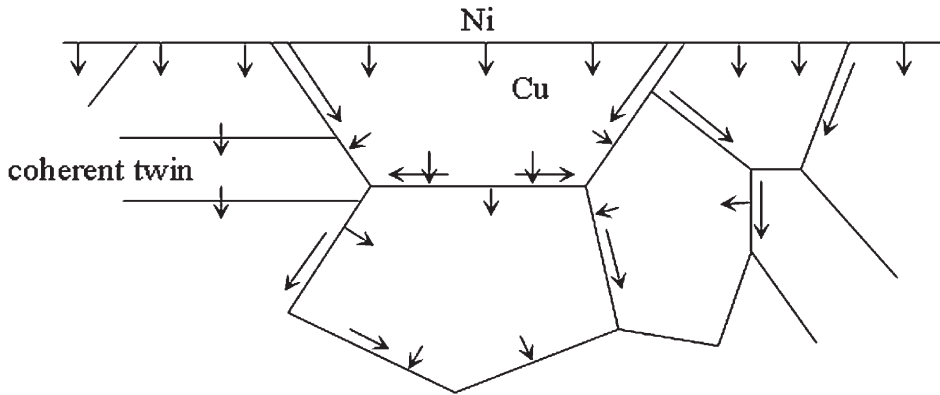
Fig. 9.   A schematic diagram illustrating the combined effects of grain boundary diffusion and volume diffusion. The relative diffusion lengths are represented by the length of the arrow (adapted from Figure 12.21 in Reed-Hill).
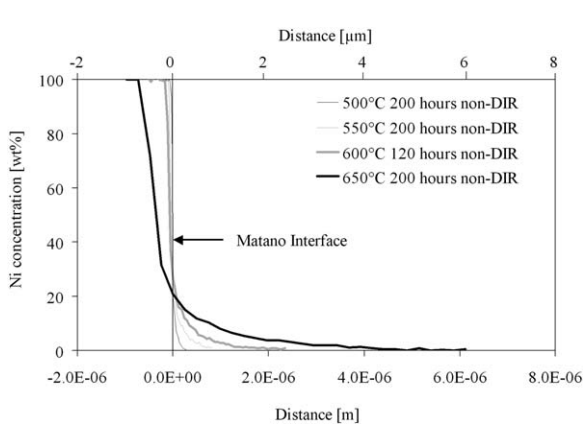

Fig. 10.   A B/M plot of non-DIR diffusion profiles from samples annealed at 500, 550, and 650 °C for 200 h and 600 °C for 120 h.
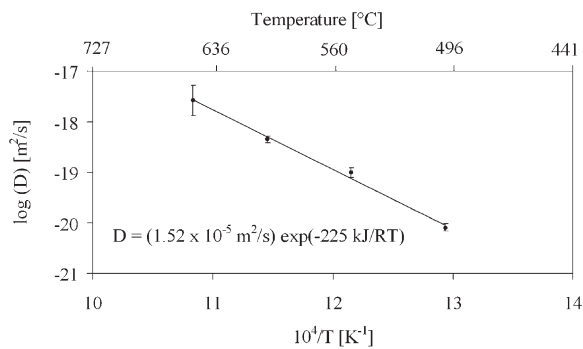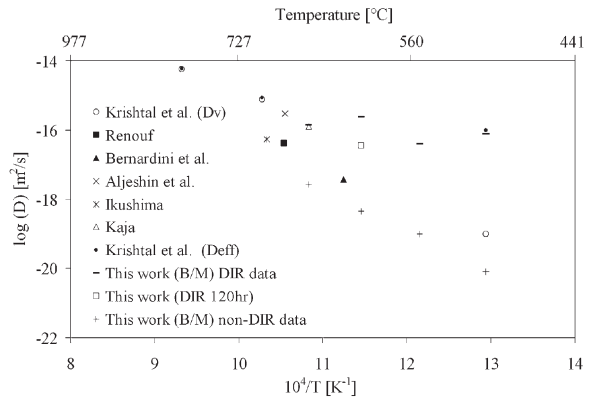

Fig. 12.   An Arrhenius plot of effective diffusivities and volume diffusivities for Ni into Cu comparing results from this work and previous work from the literature.

Fig. 11.   An Arrhenius plot of the intrinsic diffusivity of Ni in Cu calculated at [Ni] = 1 wt% using the data from the non-DIR samples from Fig. 10.

ing the "true" volume diffusion must take into consideration the influence of these new grain boundaries. Otherwise, the resulting volume diffusion will overestimate the true value. The failure to identify the impact that DIR has on determining the true volume diffusion may not be attributed to the methods previously used to extract diffusion results. For example, techniques such as autoradiography, EPMA, SIMS, or other such sectioning type techniques may not reveal microstructural information about the diffusion couple. Failure to identify DIR could result in misinterpreting effective diffusivity for volume diffusivity. Hart [1] was the first to represent the significance grain boundary diffusion contributed to volume diffusion in the

bulk (Eq. (1)). Essentially, the new grain boundaries formed by DIR increase the diffusion flux through the bulk producing an effective diffusivity that would be greater than the volume.

Volume diffusivities previously reported in the Cu-Ni system do not mention DIR [3–7]. The techniques used in previously reported volume diffusion experiments, such as EPMA and autoradiography, in the Cu-Ni system do not have the ability to detect microstructural information. Kaja [35] also studied diffusion properties in the Cu-Ni system and reported on the effective diffusivity in the Cu-Ni system. Kaja used EPMA to acquire concentration profiles, and light optical microscopy and TEM for microstructural information, and specifically mentioned that DIR and the related diffusion induced grain boundary migration occurred in this system. Kaja used polycrystalline samples diffusion annealed at 650 °C for 20 h and determined the effective diffusivities (D_{eff}) of Ni in Cu to be 2.14E-16 m²/s, 9.48E-17 m²/s, and 2.06E-16 m²/s, for 20, 50, and 80 at% Ni, respectively [35]. Fig. 13 compares the results from Kaja [35] with those calculated in this study, and shows an approximate one order of magnitude difference between the two results. The possible reason for the difference is due to the grain size. Kaja used polycrystalline samples with an average grain size of ~25 μm. In this study, the grain size in the DIR region was ~10 μm. A decrease in grain size in a polycrystalline material results in an increase in grain boundaries, and since grain boundary diffu-

sivity is dominant over volume diffusivity, the effective diffusivity increases. This was illustrated by Kaja as in Fig. 14 which shows an Arrhenius plot of effective diffusivity as a function of grain size in a polycrystalline sample. Note that as the grain size decreases, the effective diffusivity increases. Note also that the non-DIR data in Fig. 13 yields the lowest diffusion values by at least three orders of magnitude which is consistent with Kaja's work where grain boundaries contribute to the diffusion coefficient.

Not only is the choice of technique to gather volume diffusion data crucial but the method of interpreting the data is of equal importance. Such may be the case when using the B/M method to determine the volume diffusion when the microstructure consists of multiple grains. In the B/M method, there is no consideration of how the material diffuses, i.e., whether it is along grain boundaries or through the bulk. Calculating the volume diffusivity using the B/M method could overlook DIR effects and therefore produce volume diffusivities that are more characteristic of the effective diffusivity. Errors that may affect the accuracy of the B/M method include grain size, location of the interface, and location of the tangent [14]. Rhines and Mehl [14] explain that at the extreme concentration limits, where the penetration curves approach the parallelism with the distance axis, little confidence can be placed in the values
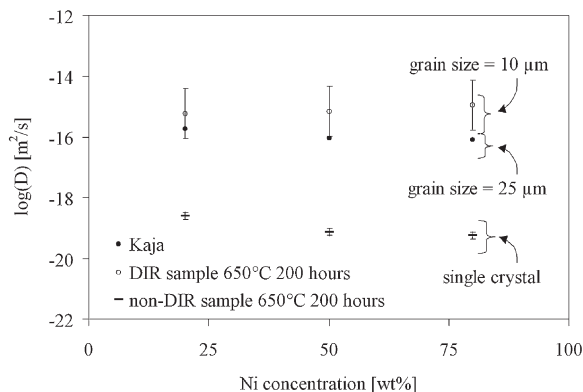

Fig. 13. A comparison of reported chemical diffusivities (D) [35] of the Cu-Ni system with results calculated in this study.
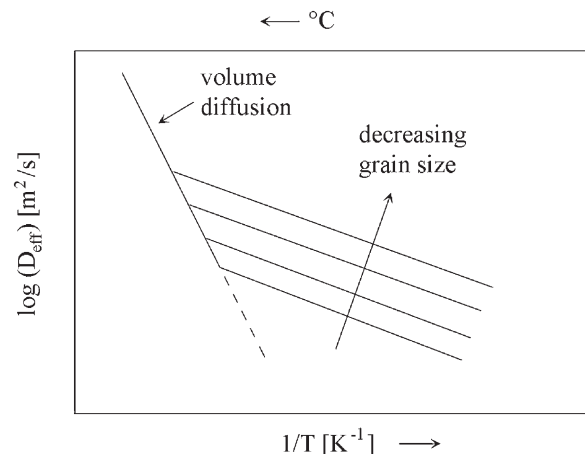

Fig. 14. An Arrhenius plot of volume and effective diffusivities as a function of grain size. Adapted from Kaja [35].

of the estimated tangents. A mathematical simplification of the B/M method, provided by Den Broeder [36], avoids the need to locate the Matano interface. However, in this work errors were also related to the inability to accurately determine the slope at either very low or very high concentrations values (i.e., near 0 and near 100 wt%), similar to that of the B/M method.

There may be another reason for the difference in activation energies between the B/M data and the published data. Note that in Fig. 12 that the published volume diffusion results are at $T > 0.6T_m(Cu)$. When $T > 0.6T_m$ grain boundary diffusion no longer dominates volume diffusion. Krishtal et al. [3] also pointed out that increasing temperatures decreases the effect of grain boundary diffusion as it pertains to effective diffusivity or bulk diffusion in polycrystalline material. Hence, by performing volume diffusion experiments at temperatures greater than $0.6T_m$, the effects of grain boundary diffusion are reduced to the point where grain boundary diffusion is not as significant. This was confirmed by Krishtal et al [3]. who showed for diffusion experiments performed on the Cu-Ni system at 700 and 800 °C the effects of grain boundary diffusion were significantly reduced compared to their results at 500 °C. Even if DIR is present, diffusion experiments conducted at $T > 0.6T_m$, may have resulted in a type A kinetics regime. Under the type A kinetics regime either the magnitude of volume diffusion is comparable to grain boundary diffusion or the grains are small enough to allow grain boundary diffusion profiles to overlap [37]. Therefore, to determine volume diffusivity, it would be an advantage to conduct the experiments at either extremely high or, preferably, low temperatures [3]. At medium temperatures the contributions of the two types of diffusion are comparable in magnitude and the experimentally determined diffusion coefficients are then "effective" ones [3].

Chen and King showed that the amount of surface coverage with new DIR grains was strongly dependent upon the amount of material removed from the surface by chemical polishing, and suggested that the nucleation of the new grains was a result of the damage from mechanical polishing [38]. The presence of DIR along the interdiffusion

zone in the five samples may suggest that electropolishing had not been performed long enough to prevent DIR. No measurements were taken to monitor the amount of Cu removed during the electropolishing step. Hence, no knowledge of residual damage from the mechanical procedures was known a priori. Evidence of DIR in the five samples may suggest that recrystallization in the interdiffusion zone was caused by the residual stress from the polishing operation. Hence, from this study, it appears that interfacial coherency strains play a large role in the formation of DIR.

The research presented herein shows how the presence (or absence) of DIR influences volume diffusion measurements, which in turn may have far reaching implications in the determination of grain boundary diffusion. Since the grain boundary activation energy depends critically on an accurate measure of the volume diffusion, a one order of magnitude change in the volume diffusivity yields a change greater than a factor of three in the grain boundary diffusivity. Thus, erroneous grain boundary diffusivities may be linked to misinterpreted volume diffusivities.

5. Conclusion

The B/M method was used to extract the volume diffusivity of Ni into Cu at 1 wt% Ni from regions experiencing DIR and regions devoid of DIR (i.e., any grain boundary contributions). The volume diffusivity for Ni in Cu for the DIR data was determined to be, $D = (3.61E-14 \ m^2/s) \exp(-41.2 \ kJ/RT)$ in the temperature range 500–650 °C. The volume diffusivity for Ni in Cu for the non-DIR data was determined to be, $D = (1.52E-5 \ m^2/s) \exp(-225 \ kJ/RT)$ in the same temperature range. The presence of DIR along the Cu-Ni interdiffusion zone resulted in more than one order of magnitude variation in the calculated effective diffusivity for samples annealed at the same temperature.

The presence of DIR influences the grain boundary diffusion results through the determination of the effective volume diffusivity. Since DIR potentially existed for all previously reported cases of volume diffusion in the Cu(Ni) system, and sub-

sequent determination of grain boundary diffusion measurements, the possibility exists that many of the intrinsic D's reported in the literature are actually uncorrected effective D's which are dependent on grain boundary contributions. Thus, this work implies that a "true" value of the volume diffusivity of Ni into Cu has been determined, and suggests that all previously reported values may be uncorrected effective diffusivities that vary with grain size. The effect of DIR on the diffusivity in other systems is not known but the work presented herein raises questions as to grain boundary effects on other volume diffusivity values.

Acknowledgements

References

[1] Hart EW. Acta Metall 1957;5:597.

[2] Hassner A. Neue Hutte 1967;12:161.

[3] Krishtal MA, Shcherbakov LM, Mokrov AP, Markova NA. Fiz Metal Metalloved 1970;29(2):305.

[4] Bernardini J, Cabane J. Acta Metallurgica 1973;21:1571.

[5] Aljeshin AN, Prokofjev SI. Poverkhnost, Fizika, Khimiya, Mechanika 1986;9:131.

[6] Renouf TJ. Phil Mag 1970;22:359.

[7] Ikushima A. J Phys Soc Japan 1959;14:1636.

[8] Levitskaya MA, Gogel'son RL. Izv Vuzou Chernaya metallurgiya 1960;3:117.

[9] Kawanami Y, Nakano M, Kajihara M, Mori T. Materials transactions. JIM 1998;39(1):218.

[10] den Broeder FJA, Nakahara S. Scripta Metallurgica 1983;17:399.

[11] Mittemeijer EJ, Beers AM. Thin Solid Films 1980;65:125.

[12] Liu D, Miller WA, Aust KT. Defect and Diffusion Forum 1989;66-69:735.

[13] Yamamoto Y, Kajihara M. Materials transactions. JIM 2001;42(8):1763.

[14] Rhines FN, Mehl RF. Trans AIME 1938;128:185.

[15] Chen F-S, King AH. Scripta Metallurgica 1986;20(10):1401.

[16] Chongmo L, Hillert M. Acta Metall 1982;30:1133.

[17] Schwarz SM, Houge EC, Giannuzzi LA, King AH. Journal of Crystal Growth 2001;222(1-2):392.

[18] Boltzmann L. Wiedemann's Ann Phys 1894;53:959.

[19] Matano C. Japan Journal of Physics 1933;8:109.

[20] Giannuzzi LA, Drown JL, Brown SR, Irwin RB, Stevie FA. Specimen prepararion in materials for TEM analysis. IV Mater Res Soc 1997. p. 19–27.

[21] Kamino T, Yaguchi T, Ohnishi T, Umemura K, Tomimatsu S. Microscopy and Microanalysis, Supplement 2 Proceedings 2000;6:510.

[22] Cliff G, Lorimer GW. Journal of Microscopy 1975;103(2):203.

[23] Williams DB, Carter CB. Transmission electron microscopy: A textbook for materials science. New York: Plenum, 1996.

[24] Glicksman ME. Diffusion in solids field theory, solid-state principles, and applications. New York: John Wiley & Sons, Inc., 2000.

[25] Reed-Hill RE, Abbaschian R. Physical metallurgy principles. Boston: PWS Publishing, 1994.

[26] Monma K, Suto H, Oikawa H. Nippon Kinsoku Gakkaishi 1964;28:192.

[27] Helfmeier H, Feller-Kniepmeier M. Journal of Applied Physics 1970;41:3202.

[28] Taguchi O, Iijima Y, Hirano K. Journal of the Japan Institute of Metals 1984;48:20.

[29] Monma K, Suto H, Oikawa H. Nippon Kinsoku Gakkaishi 1964;28:188.

[30] Ikushima A. Journal of the Physical Society of Japan 1959;14:1636.

[31] Mackliet CA. Physic Review 1958;109:1964.

[32] M.P. Macht, V. Naundorf, and R. Dohl, Proceedings of int conf on diffusion in metals and alloys at Tihany, Hungary, In: Kedves FJ, Beke DL, editors. Diffusion and Defect Monograph Series No. 7, Switzerland: Trans. Tech. Pub.; 1983. p. 516–518.

[33] Monma K, Suto H, Oikawa H. Nippon Kinsoku Gakkaishi 1964;28:192.

[34] Kaur I, Mishin Y, Gust W. Fundamentals of grain and interphase boundary diffusion. New York: Wiley, 1995.

[35] Kaja S, Ph. D. Thesis, The Pennsylvania State University, 1985.

[36] den Broeder FJA. Scripta Metallurgica 1969;3:321.

[37] Kaur I, Mishin Y, Gust W. Fundamentals of grain and interphase boundary diffusion. New York: Wiley, 1995.

[38] Chen F-S, King AH. Scripta Metallurgica 1987;21:649.